Materials Science and Engineering A 496 (2008) 214–216

Contents lists available at ScienceDirect

Materials Science and Engineering A

journal homepage: www.elsevier.com/locate/msea

Effect of Co addition on crystal structure and mechanical properties of $Ti_{0.5}CrFeNiAlCo$ high entropy alloy

F.J. Wang, Y. Zhang*

State Key Laboratory for Advanced Metal and Materials, University of Science and Technology, Beijing 100083, China

ARTICLE INFO

Article history:
Received 9 April 2008
Received in revised form 6 May 2008
Accepted 6 May 2008

Keywords:
High entropy alloy
Solid solution
Atomic packing efficiency

ABSTRACT

A high entropy alloy of $Ti_{0.5}CrFeNiAlCo$ can form two BCC crystal structures, one is with larger lattice parameter, and another with smaller one. In this paper, more Co was added in the $Ti_{0.5}CrFeNiAlCo$ alloy to detect the crystal structure and the properties changes. It is found that, with the increase of Co addition, the smaller BCC prefers to transit to FCC firstly, and the compressive strength deceased slightly.

1. Introduction

Recently the strategy of equi-atomic ratio and high entropy of mixing was used for designing multi-component alloys, namely high entropy alloys [1–5]. The high entropy alloys usually form FCC and/or BCC solid solution rather than many complex phases [6]. This kind of alloy usually exhibits very high strength [5].

Our previous work reported that the high entropy alloy of $Ti_{0.5}CrFeNiAlCo$ is mainly composed of two kinds of BCC phases, and possesses excellent room temperature compressive mechanical properties, e.g. fracture strength is about 3 GPa and plastic strain limit is about 20%, which are even superior to most of the bulk metallic glasses [5]. The metal Co is very expensive, thus the optimized content in the high entropy alloy should be very important [2,7–9]. In this paper, the crystal structure and mechanical properties of the $Ti_{0.5}CrFeNiAlCo_x$ alloy were studied.

2. Experimental procedure

Alloy ingots with nominal composition of $Ti_{0.5}CrFeNiAlCo_x$ (x: molar ratio, $x = 1, 1.5, 2, 3$, denoted by Co_1, $Co_{1.5}$, Co_2 and Co_3, respectively) were prepared by arc melting mixtures of commercial-purity metals (purity better than 99 wt%) in a Ti-gettered high-purity argon atmosphere. The alloys were re-melted several times to improve homogeneity. The ingots were then re-melted under high vacuum (10^{-3} Pa) and suction cast into a water-cooled copper mould to obtain cylindrical rods of Ø5 × 70 mm. The microstructure of as-cast samples was characterized by X-ray diffraction (XRD). Samples of Ø5 × 10 mm for compressive tests were prepared and investigated at room temperature with a strain rate of $1 \times 10^{-4}\ s^{-1}$. The fracture surface and the morphology of alloys were examined by scanning electron microscope (SEM) equipped with energy-dispersive X-ray spectrometer (EDX).

3. Results and discussion

3.1. Microstructure characterization

Fig. 1 shows the XRD patterns of the as-cast samples. The Co_1 alloy has two kinds of BCC phase reflections. It is apparent that one BCC is with larger lattice parameter of 0.2913 nm and the other with smaller one of 0.2872 nm from the strongest (1 1 0) peak as marked by "1" and "2" in Fig. 1, respectively, the larger BCC phase has a higher volume percent. With the addition of more Co, the smaller BCC phase reflections disappear and FCC reflections appear. The relative intensity of BCC reflections in the latter two alloys is smaller than the ones in the former alloys, which can be ascribed to the reason that with the increase of Co element, the random occupation of variously sized atoms on lattice sites caused serious distortion of the crystal lattice, and severe X-ray scattering thus occurred on the roughed Brag diffraction plans, weakening the diffraction signals [10,11].

Here, the solid solutions like BCC and FCC are superior to intermetallic phases to form, and the number of the phases is well below

* Corresponding author. Tel.: +86 10 62334927; fax: +86 10 62333447.
E-mail address: drzhangy@skl.ustb.edu.cn (Y. Zhang).

0921-5093/$ – see front matter © 2008 Elsevier B.V. All rights reserved.
doi:10.1016/j.msea.2008.05.020

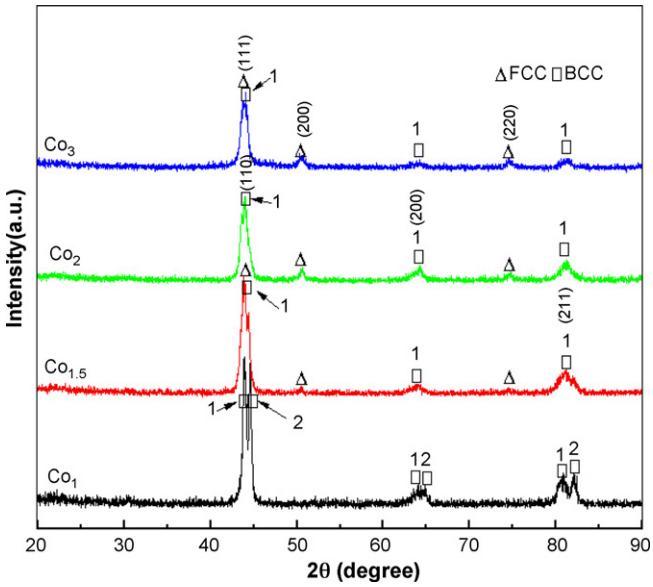

Fig. 1. XRD patterns of as-cast Co_1, $Co_{1.5}$, Co_2 and Co_3 alloys, the peaks of the big BCC is marked by "1", and the small one is marked by "2".

Table 1
Chemical composition of as-cast $Co_{1.5}$, Co_2 and Co_3 alloys (at%)

Alloy	Region	Al	Ti	Cr	Fe	Co	Ni
$Co_{1.5}$	Dendrite	24.26	7.78	12.28	13.24	24.24	18.19
	Interdendrite	13.07	9.86	20.76	17.82	24.06	14.43
Co_2	Dendrite	22.97	6.99	11.94	12.52	29.50	16.07
	Interdendrite	11.89	7.73	18.92	17.29	30.73	13.44
Co_3	Dendrite	21.16	5.98	10.60	11.21	37.43	13.62
	Interdendrite	8.53	5.05	17.08	15.05	41.80	12.49

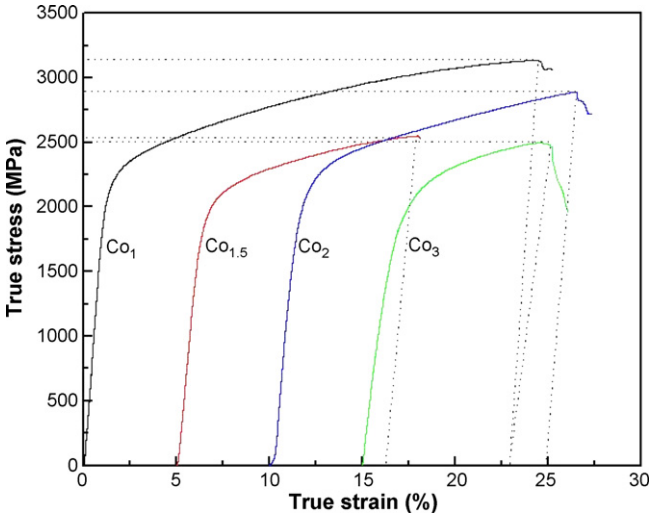

Fig. 3. Compressive true stress–strain curves of Co_1, $Co_{1.5}$, Co_2 and Co_3 alloy rods with diameter of 5 mm.

the maximum equilibrium number predicted by Gibbs phase rule, which are mainly due to the effect of the high entropy of mixing [1].

Fig. 2 shows the SEM backscattered electron images. The primary phases of all the alloys exhibit a typical cast dendrite structure and possess similar morphology. For $Co_{1.5}$, Co_2 and Co_3 alloys, the matrix is composed of primary dendrite phase, chrysanthemum-shaped eutectic structure and inter-dendrite phase, and the average arm width is about 30 μm. In Fig. 2 the big BCC, small BCC, and FCC phases are marked by "1", "2", and "3", respectively. It can be seen, with the Co addition the smaller BCC phase transforms into FCC phase, which in consistent with the XRD analysis. From the EDX analysis (listed in Table 1), the distribution of Co element is almost identical in the dendrite region and interdendrite region. The Ni and Al are rich in the dendrite, while the Ti, Cr, and Fe are rich in the interdendrite.

According to the analysis of XRD and SEM, it may be reasonable to consider that, with more Co added, the small BCC transforms into

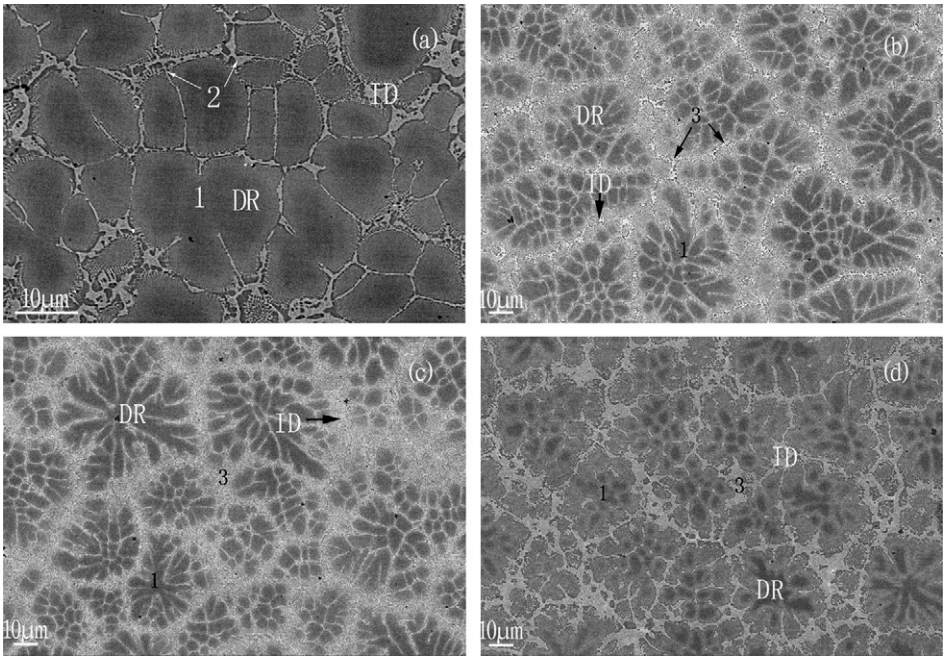

Fig. 2. SEM backscattered electron images of as-cast (a) Co_1, (b) $Co_{1.5}$, (c) Co_2 and (d) Co_3 alloys. The phase of big BCC, small BCC, and FCC was marked by "1", "2", and "3", respectively (DR: dendrite, ID: interdendrite).

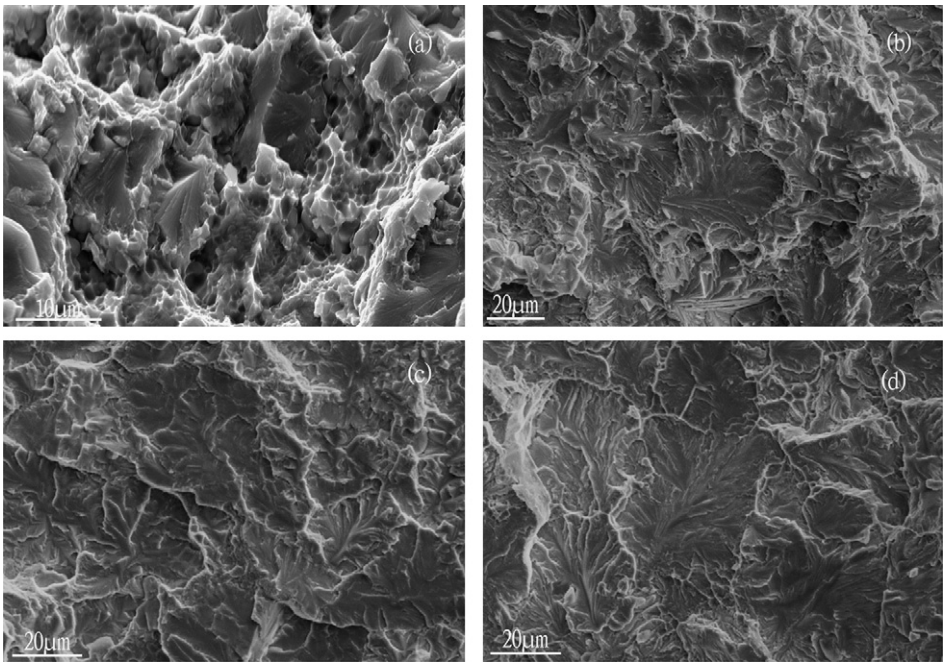

Fig. 4. SEM secondary electron images of fracture surfaces of (a) Co_1, (b) $Co_{1.5}$, (c) Co_2, and (d) Co_3 alloys.

FCC, it should be noted that the BCC structure has lower atomic packing efficiency (APE) than that of FCC. This indicates that the addition of Co atoms, will facilitate the formation of the structure with higher APE, namely FCC phases, and the smaller BCC prefers to transit to FCC first.

3.2. Compressive mechanical properties

Fig. 3 shows the compressive true stress–true strain curves of the rod samples. It is noticeable that Co_1 alloy possesses excellent room-temperature compressive mechanical properties with high strength of 3.14 GPa and large ductility of 23.3%. Compared to Co_1 alloy, both the strength and the ductility of the other three alloys decreases slightly by Co addition, anyway the mechanical properties are still superior to most of bulk metallic glasses [7]. For all the three alloys, Co_2 alloy exhibits better integrated mechanical properties with fracture strength of 2.89 GPa and ductility of 15%.

The fracture surfaces are presented in Fig. 4. The high-density dimple-shaped structures can be clearly observed in Fig. 4(a), which would be the results of the better ductility of Co_1 alloy. While for $Co_{1.5}$, Co_2 and Co_3 alloys (as shown in Fig. 4(b)–(d)), the rough facets and river-like patterns indicate the fracture morphology of alloys exhibit to be typical cleavage fracture, and the flat fracture of Co_3 alloy in Fig. 4(d) indicates its poor ductility.

The higher strength of the alloys is attributed to the solid solution strengthening mechanism of large atoms like Ti and Al in this alloy series, which occupy the lattice sites, leading to serious lattice distortion, thus enhance the effect of solid solution strengthening greatly [12].

4. Conclusion

The high entropy alloy of $Ti_{0.5}CrFeNiAlCo_x$ forms two BCC structures, one is a big BCC, and the other is a small one. With more Co addition, the small BCC prefers to transit to FCC structure first. This is due to the FCC has higher APE, the transition facilitates the relaxation of the lattice distortion energy.

References

[1] J.W. Yeh, S.K. Chen, S.J. Lin, J.Y. Gan, T.S. Chin, T.T. Shun, C.H. Tsau, S.Y. Chang, Adv. Eng. Mater. 6 (2004) 299.
[2] X.F. Wang, Y. Zhang, Y. Qiao, G.L. Chen, Intermetallics 15 (2007) 357.
[3] Y.J. Zhou, Y. Zhang, Y.L. Wang, G.L. Chen, Mater. Sci. Eng. A 454–455 (2007) 260.
[4] B. Cantor, I.T.H. Chang, P.K. night, A.J. Vincent, Mater. Sci. Eng. A 375 (2004) 213.
[5] Y.J. Zhou, Y. Zhang, Y.L. Wang, G.L. Chen, Appl. Phys. Lett. 90 (2007) 181904.
[6] A.L Greer, Nature 366 (1993) 303;
Y. Zhang, Y.J. Zhou, J.P. Lin, G.L. Chen, P.K. Liaw, Adv. Eng. Mater. 10 (2008) 534.
[7] Y.J. Zhou, et al., J. Alloys Compd. 466 (2008) 201.
[8] C.J. Tong, Y.L. Chen, S.K. Chen, J.W. Yeh, T.T. Shun, C.H. Tsau, S.J. Lin, S.Y. Chang, Met. Mater. Trans. A 36 (2005) 881.
[9] C. Min, L. Yuan, L. Yanxiang, C. Xiang, Acta Metall. Sin. 43 (2007) 1020–1024.
[10] B.D. Cullity, in: M. Cohen (Ed.), Elements of X-ray Diffraction, 2nd ed., Addison-Wesley, Reading, MA, 1978, pp. 135–139.
[11] P.H. Dederichs, Phys. Rev. B 4 (1971) 1041–1050.
[12] J.J. Harwood, Proceedings of the ASM Seminar Strengthening mechanisms in Solids, Metals Park, OH, 1960, p. 23.